Electronic Supplementary Material (ESI) for Dalton Transactions.
This journal is © The Royal Society of Chemistry 2019

Ca-, Sr-, and Ba-Coordination Polymers based on Anthranilic Acid via Mechanochemistry

Abdal-Azim Al-Terkawi[1, 2, 3], Gudrun Scholz[1], Carsten Prinz[2], Franziska Emmerling[1, 2], Erhard Kemnitz[1]

[1]Department of Chemistry, Humboldt-Universität zu Berlin, Brook-Taylor-Str. 2, D – 12489 Berlin, Germany.

[2]Federal Institute for Materials Research and Testing (BAM), Richard-Willstätter- Str. 11, D – 12489 Berlin, Germany.

[3]Institut des Biomolécules Max Mousseron (IBMM), UMR 5247, Université de Montpellier, Centre national de la recherche scientifique (CNRS), Place Eugène Bataillon, 34095 Montpellier cedex 5, France.

Supporting Information

Materials and Synthesis

Materials: Commercially accessible powders of $Ca(OH)_2$, $Sr(OH)_2$, $Sr(OH)_2{\cdot}8H_2O$, $Ba(OH)_2$, and $Ba(OH)_2{\cdot}8H_2O$ (Aldrich, chemical purity 96% - 97%) were used as inorganic precursors. Anthranilic acid (*o*ABAH, Aldrich, chemical purity 96%) was used as an organic linker. All chemicals were used without further purification.

Synthesis: All products were synthesized by milling the metal hydroxide samples and anthranilic acid with an applied molar ratio of 1 : 2, respectively. A typical time for milling was 1 h.

$\{[Ca(o\mathrm{ABA})_2(H_2O)_3]\}_n$ **(1):** was synthesized by milling $Ca(OH)_2$ + 130 µL H_2O and *o*ABAH.

$\{[Sr(o\mathrm{ABA})_2(H_2O)_2]{\cdot}H_2O\}_n$ **(2):** was obtained by milling $Sr(OH)_2{\cdot}8H_2O$ and *o*ABAH.

$\{[Ba(o\mathrm{ABA})_2(H_2O)]\}_n$ **(3):** was obtained by milling $Ba(OH)_2{\cdot}8H_2O$ and *o*ABAH.

Methods

Planetary Mill: All mechanochemical reactions were performed in a commercial planetary mill “Pulverisette 7 premium line” (Fritsch, Germany) under access to air. Each silicon nitride grinding bowl (volume: 45 ml) was filled with 1 g of a powder mixture and assembled with five silicon nitride balls (12 mm in diameter, 2.8 g each). A ball to powder mass ratio of 14 was ensured. All samples were milled with a rotational speed of 600 rpm.

Powder X-ray diffraction: Powder X-ray diffraction measurements were performed with a D8 Discover diffractometer (Bruker AXS, Karlsruhe, Germany) operated in transmission geometry with Cu-$K_{\alpha1}$ radiation (λ = 1.54056 Å, step scan: 0.009°, step time: 5 s), equipped with a Lynxeye detector. Samples were prepared in glass capillaries (diameter 0.5 mm) and were measured in a 2θ range of 5° - 65°for 35 h.

Powder X-ray diffraction diffractograms of the Ba-containing samples were recorded on a STOE Stadi MP diffractometer (STOE & Cie. GmbH, Darmstadt, Germany) operated in transmission geometry with Mo-$K_{\alpha1}$ radiation (λ = 0.709300 Å, step scan: 0.015° PSD step 0.45°, 300 s/PSD step), equipped with a Dectris Mythen 1 K linear silicon strip detector and Ge(111) double-crystal monochromator in a Bragg-Brentano geometry. The sample was measured in a 2θ range of 1° - 50° for 16 h. Reflections were compared with diffractograms of the JCPDS-PDF database.[1]

The Rietveld refinements were performed using TOPAS software (Bruker AXS).[2] The cell parameters and refinement factors are given in **Table S1**. Wherein, R_p and R_{wp} values refer to the Rietveld criteria of fit for profile and weighted profile defined by Langford and Louër.[3]

Elemental Analysis: An EURO EA equipment (HEKAtech GmbH) was used for carbon and hydrogen content determinations.

Thermal analysis: Thermogravimetry (TG) and differential thermal analysis (DTA) measurements were performed simultaneously on a thermobalance TAG 24 (SETARAM, Caluire, France). For this purpose, the samples (initial mass ≈ 12 mg) were filled into 100 µl corundum-crucibles with corundum cover and heated under a flow of argon and synthetic air at a rate of 10 K/min up to 1000 ˚C. For simultaneous analysis of evolved gasses, a mass spectrometer (Balzers Quad-star 421) was coupled by a heated (180 ˚C) quartz glass capillary (measurements were performed in MID (multiple ion detection) mode.

Magic Angle Spinning NMR: ^1H and $^1H\text{->}^{13}C$ CP MAS NMR spectra were recorded on a Bruker AVANCE 400 spectrometer (Larmor frequencies: ν_{1H} = 400.1 MHz and ν_{13C} =100.6 MHz) using both a 2.5 mm and a 4 mm double-bearing magic angle spinning (MAS) probe (Bruker Biospin). ^1H MAS studies were recorded with a $\pi/2$ pulse length of 3.6 μs and a recycle delay of 5 s. Values of the isotropic chemical shifts of ^1H and ^{13}C are given with respect to TMS. A contact time of 10 ms was used for the $^1H\text{->}^{13}C$ CP MAS NMR experiments.

Attenuated Total Reflection-Infrared Spectroscopy (ATR-IR): Infrared spectra were measured using an Equinox 55 FT-IR spectrometer (Bruker, Ettlingen, Germany) with a spectral resolution of 2 cm^{-1} averaging over 100 scans. A CaF_2 window is used.

Gas Sorption: Gas adsorption experiments were carried out on an ASAP 2010 (Micromeritics, Norcross, USA). Nitrogen was used as an adsorptive at a temperature of 77 Kelvin. Prior to the measurements, samples were degassed at room temperature and 200 ˚C for 24 h in vacuum. Specific surface areas were calculated by Brunauer-Emmett-Teller (BET) method.[4,5] with a molecular sectional area of 0.162 nm² according to ISO 9277 (2010).[6]

Dynamic vapor sorption: The experiments of water and n-octane dynamic vapor sorption (DVS) were performed on the DVS-1 instrument (Surface Measurements Systems, London, UK). The DVS System is a gravimetric sorption apparatus consists of a thermostated sample chamber for setting a constant temperature of the sample and a flow controller for producing a controllably variable vapor pressure. The adsorbed mass is determined by continuous weighing as a function of the relative pressure. The isotherms were measured over a range of 0 – 98% relative humidity (RH) at a temperature of 25˚C.

X-ray Absorption Spectroscopy: The EXAFS (extended X-ray absorption fine structure) spectra were recorded for the Ca element with absorption edges at 4.038 keV. Samples were measured at the B18 beamline (Diamond, Oxford UK) in Rapid Access mode. The beam was monochromatized using a double-crystal monochromator (DCM). The measurements were performed at the K edge for Ca at 4.038 keV. The measurements were acquired in a quick-EXAFS mode in the range of 3.838-5.000 keV, and a nominal step size of 0.3 eV was used. The Ca-samples were used as-synthesized, and the fine powders were fixed between two strips.

The EXAFS spectra were recorded for the Sr compounds at the Sr K edge at 16.107 keV. Samples were measured at the BAM*line* (BESSY-II, Berlin, Germany). The beam was monochromatized using a double-crystal monochromator (DCM). The measurements were performed conventionally, in which the size of the beam spot was 8x1 mm. The measurements were performed at the K edge for Sr (16.107 keV). The energy was scanned in the following manner: from -100 eV to -20 eV below the edge in 10 eV steps; from -19 eV below the edge to 20 eV above the edge in 0.5 eV steps; from 21 eV to 100 eV above the edge in 1.5 eV steps and the EXAFS range was scanned in equidistant k steps of 0.04 Å until k=14 Å. Sr-samples were diluted by boron nitride. The diluted samples were fixed in plastic sample holders between two Kapton foils. Every sample was repeatedly measured. As detectors, two ionization chambers were used for the primary beam (I_0) and the absorption of the sample (I_1), respectively.

The data treatments were carried out using the Demeter software package (Artemis & Athena). These GUIs programs belong to the software package IFEFFIT (v. 1.2.11).[7] For better assignation of the coordination number and interatomic distances, EXAFS simulations of the determined crystal structures were carried out in FEFF and compared with the measured spectra.[8]

Figures and Tables

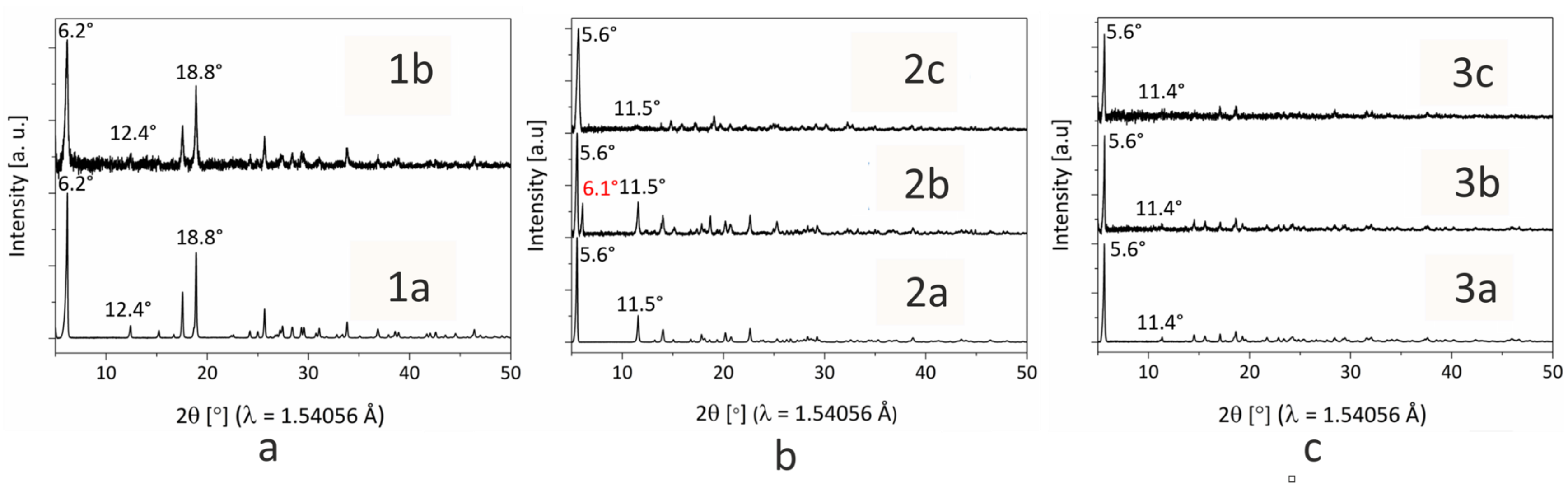

Figure S1: Powder X-ray diffraction (PXRD) patterns of compounds **1**, **2**, and **3**. **(a)** $\{[Ca(oABA)_2(H_2O)_3]\}_n$ (**1**) obtained by milling *o*ABAH with $Ca(OH)_2$ + 130 µl H_2O for 1h (1a) or 4h in the absence of water (1b). **(b)** $\{[Sr(oABA)_2(H_2O)_2]\cdot H_2O\}_n$ (**2**) obtained by milling *o*ABAH with $Sr(OH)_2\cdot 8H_2O$ for 1h (2a), $Sr(OH)_2$ + 130 µl H_2O for 1h (2b), or $Sr(OH)_2$ for 4h (2c). **(c)** $\{[Ba(oABA)_2(H_2O)]\}_n$ (**3**) obtained by milling *o*ABAH with $Ba(OH)_2\cdot 8H_2O$ for 1h (3a), $Ba(OH)_2$ + 130 µl H_2O for 1h (3b), or $Ba(OH)_2$ for 1h (3c). The molar ratio between organic and inorganic samples was maintained as 1:2, respectively.

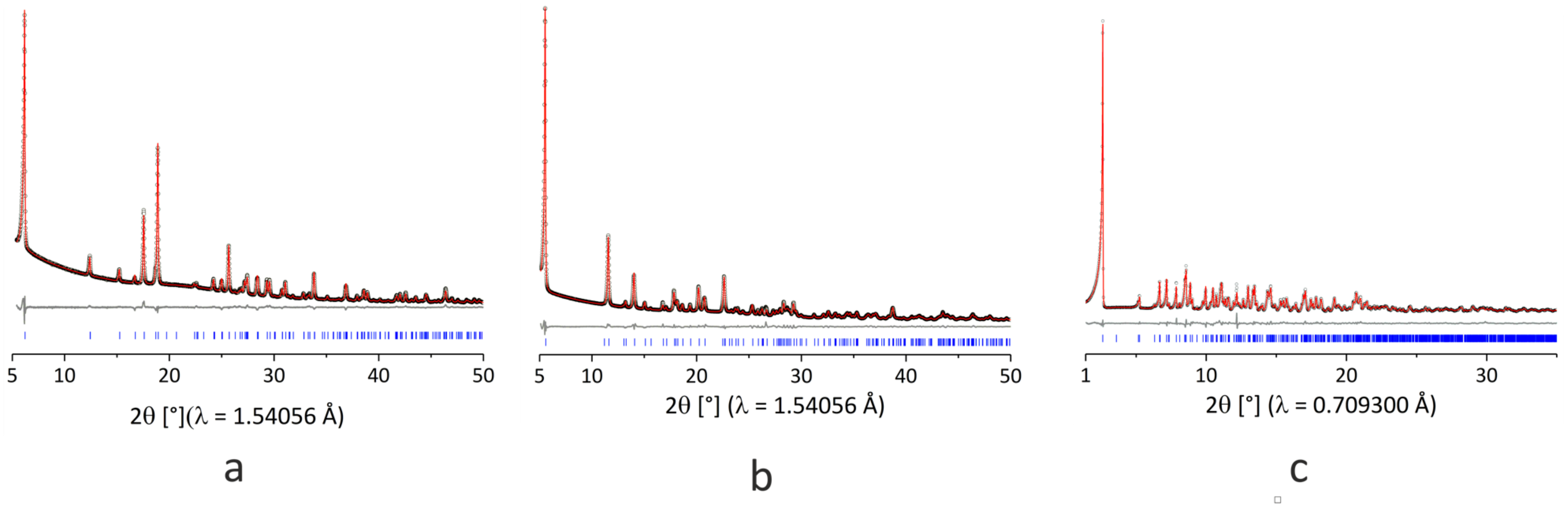

Figure S2: The results of Rietveld refinements for the structures **1** (a), **2** (b), and **3** (c). In the refined data, scattered X-ray intensity at ambient conditions is shown as a function of diffraction angle 2θ. The observed pattern (black circles), the best Rietveld fit profile (red line), the reflection positions (blue tick marks), and the difference curve (grey line) between observed and calculated profiles are shown.

Table S1: Coordination environments, crystal data, and refined parameters derived from the crystal structures of compounds **1**, **2**, and **3**.

	{[Ca(*o*ABA)$_2$(H$_2$O)$_3$]}$_n$ **(1)**	{[Sr(*o*ABA)$_2$(H$_2$O)$_2$]·H$_2$O}$_n$ **(2)**	{[Ba(*o*ABA)$_2$(H$_2$O)]}$_n$ **(3)**
C.N.	7	9	9
M-O (carboxyl)	4 (O1, O1’, O2, O2’) from 4 ligands	5 (O1, O1’, O2, O2’, O3) from 4 ligands	6 (O1, O1’, O2, O2’, O3, O4) from 5 ligands
M-N (amino)	-	1 (N2)	1 (N1)
Coordinating H_2O molecules	3 (O3w, O4w, O4w’)	1 terminal (O7w) + 2 bridging (O5w, O6w)	2 bridging (O5w, O5w’)
Crystal water	-	1 (O6w)	-
Coordination mode (Ligand)	2Ca (bidentate carboxyl group)	Lignad 1: 3Sr (O1, O2, N2) Ligand 2: 1Sr (O3)	Lignad 1: 3Ba (O1, O2, N1) Ligand 2: 2Ba (O3,O4)
C—O (carboxylate) (Å)	1.260(4) - 1.261(5)	1.236(1) - 1.264(1)	1.264(1) - 1.281(1)
C—N (amino) (Å)	1.399(1)	1.396(1) - 1.437(2)	1.375(1) - 1.411(1)
M^{II}—O (carboxylate) (Å)	2.331(5) - 2.378(5)	2.491(1) - 2.929(1)	2.721(1) - 3.013(1)
M^{II}—N (amino) (Å)	-	3.069(2)	3.051(1)
M^{II}—O (water) (Å)	2.413(1) -2.489(5)	2.625(2) - 2.711(2)	2.890(1) - 2.914(1)
O—M^{II}—O angle (°)	73.680(9) - 163.863(2)	46.289(4) – 148.222(3)	44.754(1) – 148.664(1)
M^{II}—(chain)—M^{II} (Å)	1D: Ca-(Ligand)-Ca = 4.706(1)	1D Sr-(O5w,O1,O1’)-Sr = 3.913(4) 1D Sr-(O6w,O2,O2’)-Sr = 3.917(4)	1D: Ba-(O5w,O1,O3)-Ba = 4.329(1) 2D: Ba-(Ligand)-Ba = 6.084(1)
M^{II}—M^{II}—M^{II} angle (°) (1D-chain)	114.721(1)	122.945(9)	129.222(1)
M^{II}···(interlayer)···M^{II} (Å)	14.2	7.832(9)	14.369(4)
Dimensionality	1D (I^0O^1)	1D (I^1O^0)	2D (I^1O^1)
Cell parameters			
Empirical formula	$C_{14}H_{18}CaN_2O_7$	$C_{14}H_{18}SrN_2O_7$	$C_{14}H_{14}BaN_2O_5$
Cell mass (g/mol)	366.38	413.92	427.6
Crystal system	Orthorhombic	Monoclinic	Orthorhombic
Space group	Pbcn (60)	C_2 (5)	Pbcn (60)
Cell volume (Å^3)	1652.17(5)	1701.62(7)	2952.23(2)
a (Å)	28.433(6)	32.085(9),	31.021(1)

	{[Ca(*o*ABA)$_2$(H$_2$O)$_3$]}$_n$ **(1)**	{[Sr(*o*ABA)$_2$(H$_2$O)$_2$]·H$_2$O}$_n$ **(2)**	{[Ba(*o*ABA)$_2$(H$_2$O)]}$_n$ **(3)**
b (Å)	7.332(1)	7.832(1),	12.167(4
c (Å)	7.926(1)	6.879(2)	7.822(2)
α, β, γ (°)	α = β = γ = 90	α = γ = 90, β = 100.157	α = β = γ = 90
Cell ratio			
a/b	3.878	4.09	2.551
b/c	0.925	1.1386	1.555
c/a	0.279	0.2144	0.252
Z	4	4	8
Density (calc.) g/cm^3	1.47	1.62	1.92
Refinement parameters			
R_{wp}	2.69	3.19	4.65
R_p	1.82	2.15	3.28
R_{Bragg}	2.213	1.166	1.863
GOF	2.31	4.30	2.95
PXRD measurements			
Instrument	D8 Discover		STOE Stadi MP
Calibration	Si standard powder		
λ (Å)	1.54056 (Cu-$K_{\alpha1}$)		0.709300 (Mo-$K_{\alpha1}$)
2θ range (°)	5 – 65		1 – 50
step size	0.009°		0.015°
Collection time	35 h		17 h

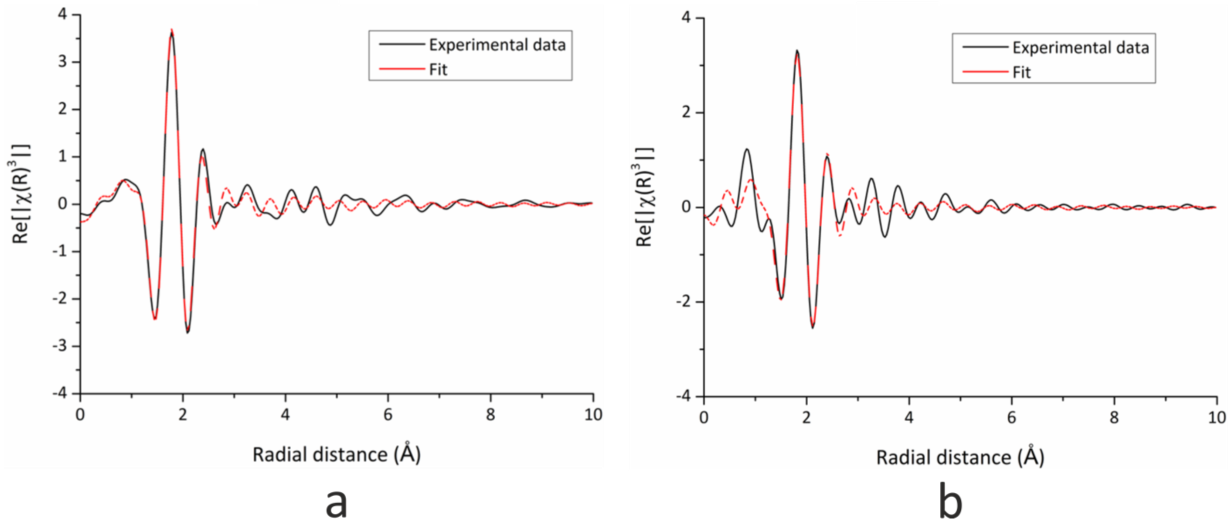

Figure S3: Ca *K*-edge EXAFS spectrum shown in real space for compounds **1** (a) and Sr- *K*-edge EXAFS spectrum shown in real space for **2** (b). The experimental data (black line) are presented along with the best fit model of the FT magnitude (red dotted line).

Table S2: EXAFS fit parameters and scattering paths for the compounds **1** and **2**.

	$\{[Ca(oABA)_2(H_2O)_3]\}_n$ (**1**)			$\{[Sr(oABA)_2(H_2O)_2]\cdot H_2O\}_n$ (**2**)			
Scattering path	R_{model} (Å)	R_{fit} (Å)	R_{diff}^2 (Å)	scattering path	R_{model} (Å)	R_{fit} (Å)	R_{diff}^2 (Å)
Ca—O1	2.33	2.32	0.0001	Sr—O1	2.93	2.91	0.0004
Ca—O1’	2.33	2.32	0.0001	Sr—O1	2.49	2.48	0.0001
Ca—O2	2.38	2.37	0.0001	Sr—O2	2.60	2.60	0
Ca—O2’	2.38	2.37	0.0001	Sr—O2	2.53	2.51	0.0004
Ca—O3w	2.41	2.41	0	Sr—O3	2.50	2.48	0.0004
Ca—O4w	2.49	2.48	0.0001	Sr—N2	3.07	3.05	0.0004
Ca—O4w’	2.49	2.48	0.0001	Sr—O5w	2.62	2.60	0.0004
Ca—O3w	2.41	2.41	0	Sr—O6w	2.71	2.70	0.0001
				Sr—O7w	2.65	2.63	0.0004
Average (Å)	2.40	2.39			2.68	2.66	
RMSE			0.000075				0.00029
R-factor	0.019				0.029		
Reduced chi-square	484.56				13460.18		

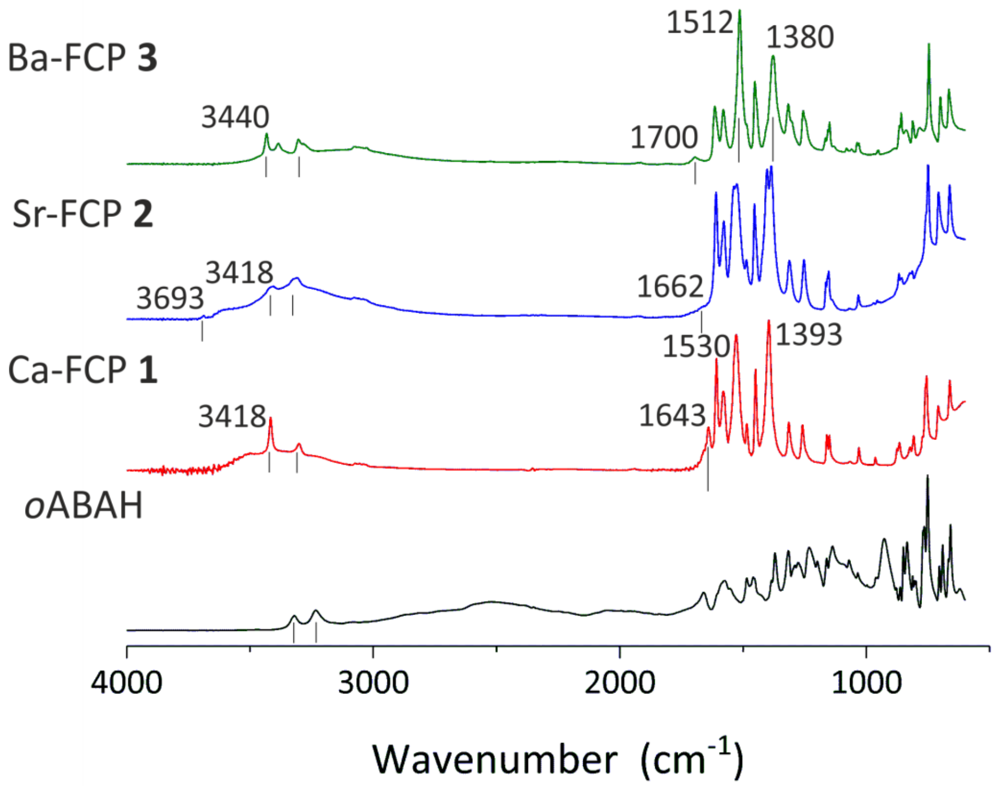

Figure S4: The ATR-IR spectra of anthranilic acid (black spectrum), Ca-CP **1** (red spectrum), Sr-CP **2** (blue spectrum), and Ba-CP **3** (green spectrum).

Table S3: The results of elemental analysis and BET surfaces area (S_{BET} m^2/g) of compounds Ca-CP (**1**), Sr-CP (**2**), and Ba-CP (**3**) as-synthesized, after thermal annealing at 200 °C, and after the controlled hydration of the dehydrated samples.

	Ca-CP			Sr-CP			Ba-CP		
	As-synthesized	1 (200 ˚C)	Controlled hydration	2	2 (200 ˚C)	Controlled hydration	3	3 (200 ˚C)	Controlled hydration
N% found (calc.)	7.6 (7.6)	8.9 (8.96)	7.8	6.1 (6.8)	7.7 (7.8)	7.4	6.5 (6.5)	6.8 (6.8)	6.8
C% found (calc.)	46.0 (45.9)	53.7 (53.8)	48.2	36.4 (40.6)	46.5 (46.7)	44.7	37.1 (39.3)	40.7 (41.0)	38.9
H% found (calc.)	4.9 (4.9)	3.8 (3.8)	4.5	4.3 (4.3)	3.2 (3.3)	3.4	3.2 (3.3)	2.8 (2.9)	3.1
S_{BET} (m^2g^{-1})	7.2 ± 0.02	6.6 ± 0.01		2.9 ± 0.01	0.3 ± 0.002		3.2 ± 0.01	0.3 ± 0.01	

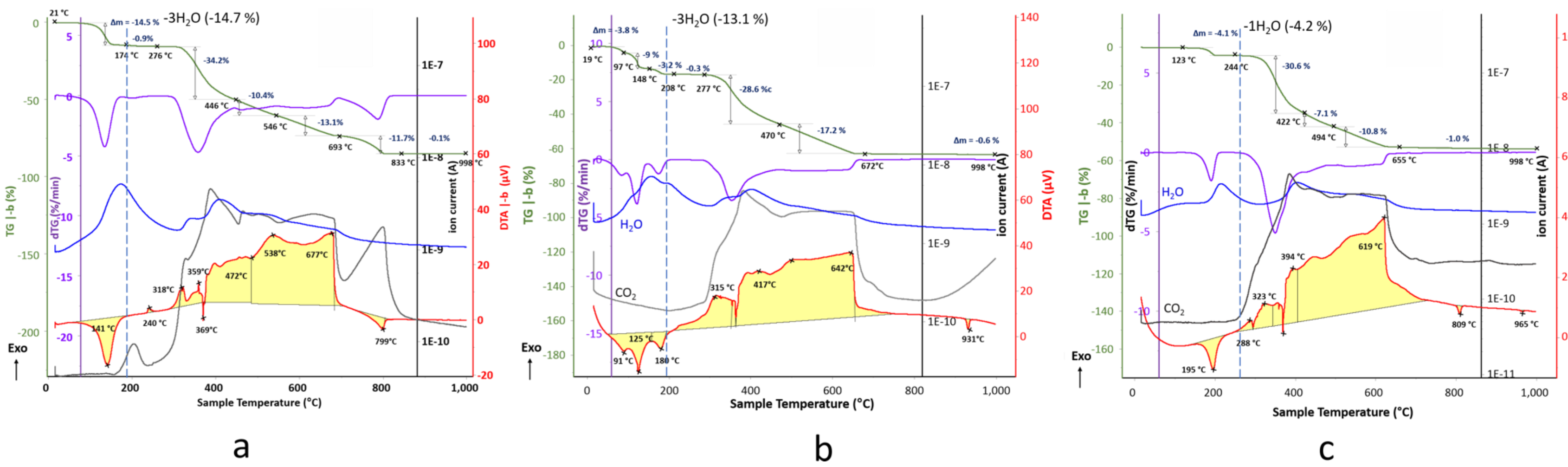

Figure S5: Thermoanalytical curves of (a) {[Ca(*o*ABA)$_2$(H$_2$O)$_3$]}$_n$ (**1**), (**b**) {[Sr(*o*ABA)$_2$(H$_2$O)$_2$]·H$_2$O}$_n$ (**2**), and (**c**) {[Ba(*o*ABA)$_2$(H$_2$O)]}$_n$ (**3**).

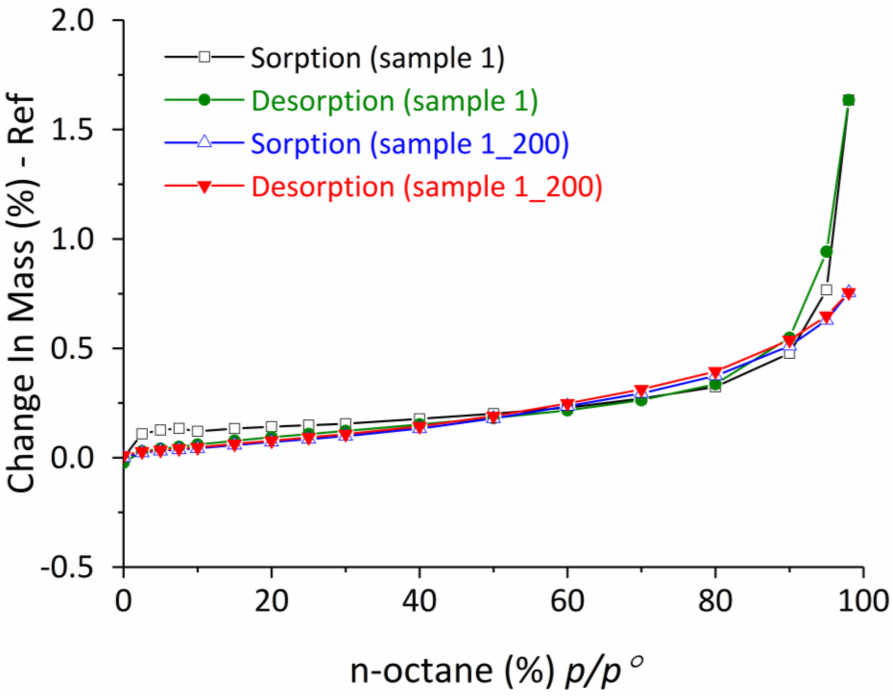

Figure S6: Isotherm curves for the dynamic vapor sorption of *n*-octane on samples of compound **1** as-synthesized (black and green isotherms) and the thermally treated sample at 200°C (blue and red isotherms)**.**

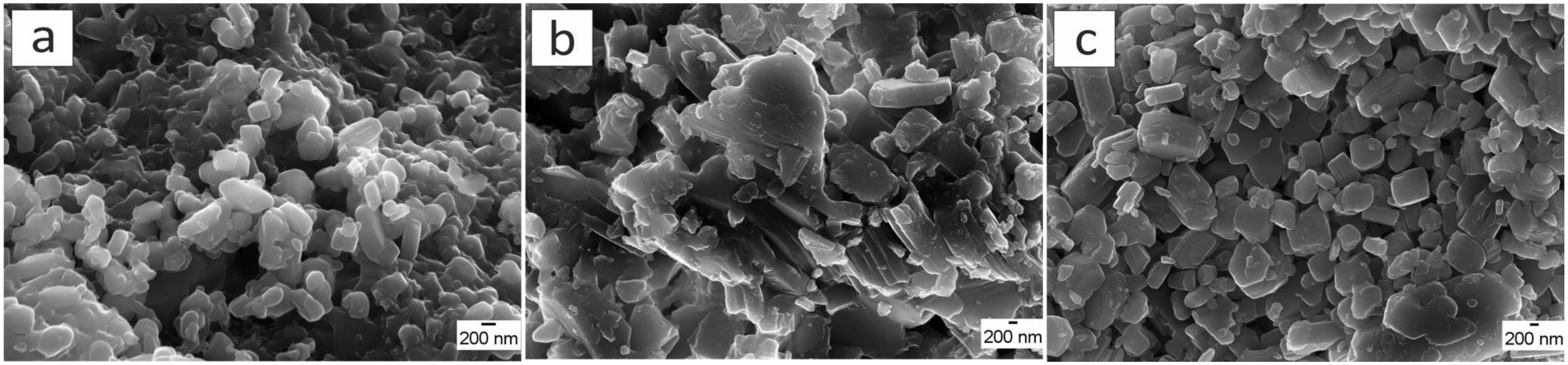

Figure S7: SEM images of (a) $\{[Ca(o\text{ABA})_2(H_2O)_3]\}_n$ (**1**), (b) $\{[Sr(o\text{ABA})_2(H_2O)_2]\cdot H_2O\}$ (**2**), and (c) $\{[Ba(o\text{ABA})_2(H_2O)]\}_n$ (**3**).

References

(1) JCPDS-ICDD, International Centre for Diffraction Data: PDF-2 Database (Sets 1–51 plus 70–89). International Centre for Diffraction Data: PA 19073–3273 USA 2001.

(2) TOPAS 5: General Profile and Structure Analysis Software for Powder Diffraction Data (User's Manual). Bruker AXS: Karlsruhe, Germany 2010.

(3) Langford, J. I.; Louër, D. Powder diffraction. *Reports Prog. Phys.* **1996**, *59* (2), 131–234.

(4) Brunauer, S.; Emmett, P. H.; Teller, E. Adsorption of Gases in Multimolecular Layers. *J. Am. Chem. Soc.* **1938**, *60* (2), 309–319.

(5) Fagerlund, G. Determination of specific surface by the BET method. *Matériaux Constr.* **1973**, *6* (3), 239–245.

(6) ISO 9277. *Determination of the specific surface area of solids by gas adsorption — BET method*; 2010; Vol. E.

(7) Ravel, B.; Newville, M. ATHENA, ARTEMIS, HEPHAESTUS: Data analysis for X-ray absorption spectroscopy using IFEFFIT. *J. Synchrotron Radiat.* **2005**, *12* (4), 537–541.

(8) Rehr, J. J.; Kas, J. J.; Vila, F. D.; Prange, M. P.; Jorissen, K. Parameter-free calculations of X-ray spectra with FEFF9. *Phys. Chem. Chem. Phys.* **2010**, *12* (21), 5503.